

Sulfur accumulation in the timbers of King Henry VIII's warship *Mary Rose*: A pathway in the sulfur cycle of conservation concern

Magnus Sandström^{*†}, Farideh Jalilehvand[‡], Emiliana Damian^{*}, Yvonne Fors^{*}, Ulrik Gelius[§], Mark Jones[¶], and Murielle Salomé^{||}

^{*}Department of Structural Chemistry, Stockholm University, SE-106 91 Stockholm, Sweden; [‡]Department of Chemistry, University of Calgary, Calgary, AB, Canada T2N 1N4; [§]Department of Physics, Ångström Laboratory, Uppsala University, P.O. Box 530, SE-751 21 Uppsala, Sweden; [¶]The Mary Rose Trust, College Road, HM Naval Base, Portsmouth, PO1 3LX, United Kingdom; and ^{||}European Synchrotron Radiation Facility, BP 220, 38043 Grenoble Cedex, France

Edited by Harry B. Gray, California Institute of Technology, Pasadena, CA, and approved August 11, 2005 (received for review May 31, 2005)

In marine-archaeological oak timbers of the *Mary Rose* large amounts of reduced sulfur compounds abound in lignin-rich parts such as the middle lamella between the cell walls, mostly as thiols and disulfides, whereas iron sulfides and elemental sulfur occur in separate particles. Synchrotron-based x-ray microspectroscopy was used to reveal this environmentally significant accumulation of organosulfur compounds in waterlogged wood. The total concentration of sulfur in reduced forms is ≈ 1 mass % throughout the timbers, whereas iron fluctuates up to several mass %. Conservation methods are being developed aiming to control acid-forming oxidation processes by removing the reactive iron sulfides and stabilizing the organosulfur compounds.

organosulfur | waterlogged wood | iron sulfides | conservation | marine archaeology

The *Mary Rose* served successfully for 35 years as a principal warship in Henry VIII's navy. In 1545, while maneuvering to engage a French fleet outside Portsmouth, she unexpectedly went down in 14 m of water with disastrous loss of life; only 30–40 survived of ≈ 400 . The wreck was rediscovered in 1971, and underwater excavations showed that approximately one-third of the hull remained (1–3). Most of the starboard side and parts of the decks had survived deeply embedded in soft yielding clay. In the strong tidal flows, the hull had served as a silt trap, contributing to the well-preserved condition of $\approx 19,000$ recovered objects. After the port side had eroded away, weakened by wood-boring organisms, a hard gray shelly layer of compacted clay was formed, effectively protecting the remaining timbers (1, 3). The hull was salvaged in 1982.

Sulfur in Marine-Archaeological Wood

Recent reports reveal that tons of reduced sulfur compounds unexpectedly had accumulated in the timbers of the almost intact hull of the 17th-century Swedish warship *Vasa* during its 333 years on the seabed in Stockholm harbor (refs. 4–8; see also references within ref. 6). The sulfur slowly oxidizes forming sulfuric acid, which if left untreated would eventually degrade the cellulose fibers by acid hydrolysis and reduce the mechanical stability of the hull timbers. Further analyses show that accumulation of reduced sulfur compounds is common in wooden shipwrecks preserved in seawater (9).

How serious a problem could this discovery be for the *Mary Rose*? Preconservation examinations of the waterlogged oak timbers established a decayed outer zone and a relatively sound inner core. To prevent shrinkage and cracking, a nonvolatile substance must replace the internal water before drying the wood. Polyethylene glycol (PEG) spray treatment, a conservation method developed for the *Vasa* (10), was started in late 1994 by recycling 30 m³ of aqueous solution of PEG 200. The low average molecular mass [≈ 200 with $n \approx 4$ for $\text{H}(\text{OCH}_2\text{CH}_2)_n\text{OH}$] facilitates penetration into the wood. The

spray treatment will continue for ≈ 5 further years, starting in 2006 with a solution of PEG 2000 to provide higher stability and make the outer decayed zone less hygroscopic after slow controlled air-drying in the final stage (3).

Sulfur and Iron Analyses

Oak wood cores ($0.4 \times 15\text{--}20$ cm) were sampled from four hull timbers and from pinewood (Fig. 1), by means of a manual increment borer. The total sulfur and iron concentrations in the dried wood were determined by several methods, x-ray photoelectron spectroscopy (5, 11), x-ray fluorescence line scans, and elemental analyses (9). For further details, see *Supporting Text* and Figs. 7–12, which are published as supporting information on the PNAS web site. In all cores the sulfur concentration varies between ≈ 0.4 and 2 mass % S throughout the timbers (Figs. 2 and 12). The analyses signify a substantial amount, at least 2 tons of sulfur, in the hull of ≈ 280 tons (3). The distribution is much more uniform than that in the *Vasa*, where bacterial degradation (12, 13) of the surface layers ($\approx 1\text{--}2$ cm) seems to be required for a high accumulation of both sulfur and iron (6–9). The iron concentration in the wood of the *Mary Rose* fluctuates considerably, from <0.1 mass % in light-colored wood to several mass % close to cracks, bolt holes, or in degraded “black oak” (Figs. 2 and 12), without the close correspondence between sulfur and iron profiles as often found for the *Vasa*.

For *in situ* determination of the characteristic sulfur species present in the wood, we recorded sulfur K-edge x-ray absorption near-edge structure (XANES) spectra for cores 1a, 2, and 3 at Stanford Synchrotron Radiation Laboratory (SSRL), using beamline 6-2 dedicated to sulfur spectroscopy for natural samples in atmospheric helium pressure (14–16). Normalized XANES spectra of sections along the oak cores are shown in Figs. 3 and 7. Principal component analysis (17) of the spectra indicates at least six significant sulfur components, with mostly four types of reduced species contributing to the major peak at 2,473 eV ($1 \text{ eV} = 1.602 \times 10^{-19} \text{ J}$). Curve fitting with XANES spectra of standard compounds (15–18) quantitatively reveals thiols (R–SH), disulfides (R–SS–R') with a characteristic double-peak, and elemental sulfur (S₈) in all samples and in core 2 also pyrite (FeS₂) in sharply varying amount (Fig. 4 and Table 1). The minor peak, visible at 2,482.4 eV throughout core 1a (magazine-stored oak) that corresponds to $\approx 5\%$ of the sulfur oxidized to sulfate (SO₄²⁻), is absent for core 2 from hull timber under spray

This paper was submitted directly (Track II) to the PNAS office.

Freely available online through the PNAS open access option.

Abbreviations: PEG, polyethylene glycol; SSRL, Stanford Synchrotron Radiation Laboratory; SXM, scanning x-ray absorption microspectroscopy; XANES, x-ray absorption near-edge structure.

[†]To whom correspondence should be addressed. E-mail: magnuss@struc.su.se.

© 2005 by The National Academy of Sciences of the USA

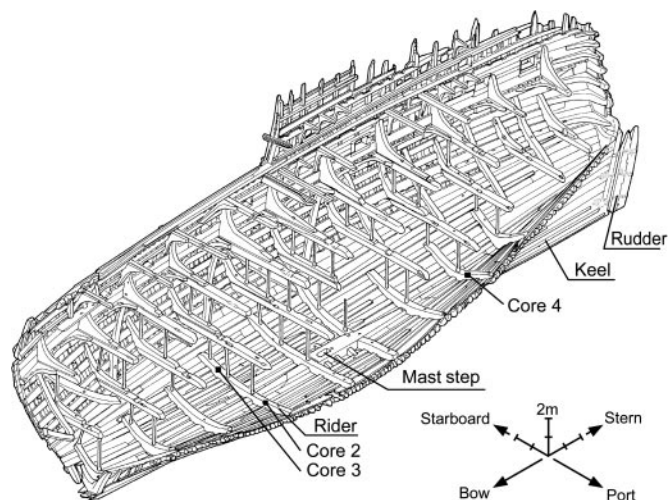


Fig. 1. Isometric of the *Mary Rose* hull showing the main constructional features, excluding decks, internal structures, and fittings. Dimensions: stem to bow, 40.9 m; breadth, 11.7 m. Sample positions are indicated for oak cores 2–4 (cores 1a, 1b, and 5 are from magazine-stored timbers).

treatment. In all XANES spectra sulfoxides [R_2SO or $R(SO)R'$] with a peak at $\approx 2,476$ eV (19) can be discerned as a minor component, a few percent of the total sulfur amount.

The energy scale of the sulfur x-ray absorption features was calibrated by assigning the first peak position of sodium thio-sulfate, $Na_2S_2O_3 \cdot 5H_2O$, to 2,472.02 eV (14). By careful appraisal of appropriate standard spectra, in particular for the overlapping reduced forms that to some extent correlate in the fitting procedure (for peak energies see *Supporting Text*), we estimate approximately $\pm 10\%$ error limits in the reported value for the relative amount of the sulfur species.

Samples also were taken from a salt-infested gunshield after conservation (Fig. 4d), originally covered with segmented iron plates that corroded away. Elemental analyses showed high total sulfur and iron content in the samples, up to 10 mass % S and 5 mass % Fe. The XANES fitting was consistent with approximately one-third of the sulfur remaining in reduced forms, mainly as pyrite. X-ray powder diffraction (XPD) confirmed pyrite and traces of mackinawite (Fe_8S_9), together with the hydrated iron sulfates, rozenite ($Fe^{II}SO_4 \cdot 4H_2O$) and melanterite ($Fe^{II}SO_4 \cdot 7H_2O$) and also some natrojarosite [$NaFe^{III}_3(SO_4)_2(OH)_6$]. Two years later, XPD showed that all reduced sulfur in the samples had oxidized to sulfates, mainly rozenite (see *The Role of Iron*, below).

Results from multielement analyses by x-ray photoelectron spectroscopy on core 1b are shown in Table 2 and Fig. 5. The

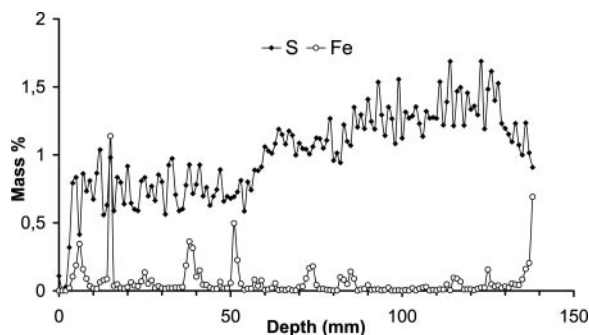


Fig. 2. Total sulfur and iron in mass % from x-ray fluorescence line scan (9) along oak core 2 from a hull rider (cf. Fig. 1).

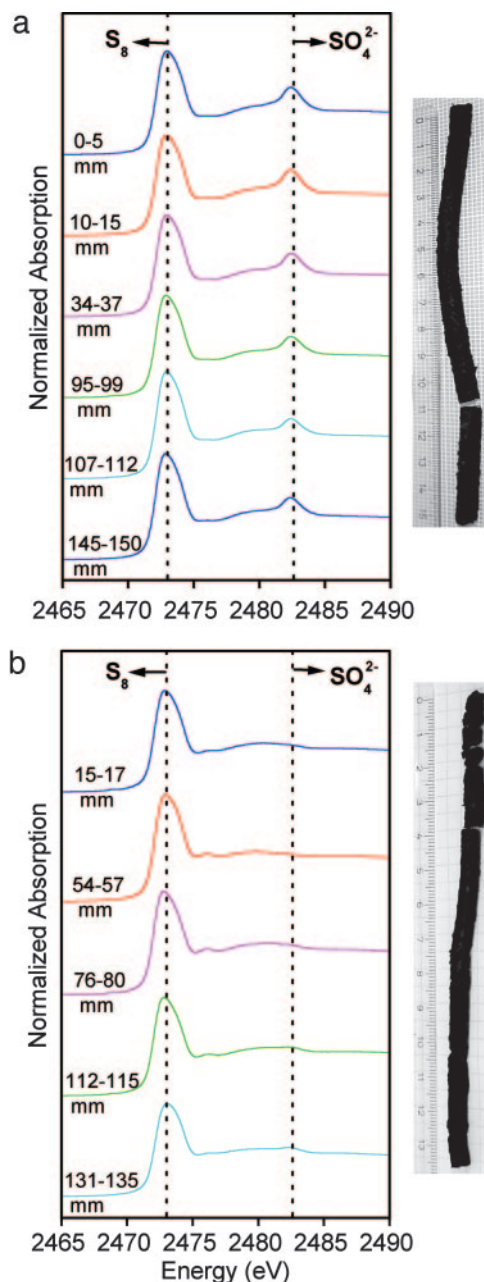


Fig. 3. Normalized sulfur K-edge XANES spectra (SSRL) from sections of oak cores from surface (0 mm) and inwards. (a) Core 1a: oak beam, magazine stored in airtight wrap. (b) Core 2: hull rider under PEG treatment. The major peak at 2,473 eV originates from reduced sulfur species (thiols $R-SH$, disulfides $R-SS-R'$, elemental sulfur S_8 , and pyrite FeS_2). The minor peak at 2,482.4 eV (core 1a) corresponds to oxidized sulfur in sulfate.

boron (≈ 0.2 mass %) found at all depths indicates efficient penetration of boric acid, $B(OH)_3$ (4–7), from a fungicide treatment before magazine storage (3). The two distinct x-ray photoelectron spectroscopy sulfur 2p peaks represent high and low oxidation states, and in addition curve fitting (Fig. 10) confirms sulfoxide as a minor intermediate. Large variations occur along the core in the carbon and oxygen concentrations with an inverse correlation (high C corresponds to low O; cf. Table 2) also shown in the relative sizes of the two C_{1s} peaks at 285.0 and 286.5 eV (Fig. 11), which mainly correspond to CH_2 (lignin) and $C-O$ (cellulose) groups, respectively. The lignin to cellulose ratio increases for wood with bacterially degraded

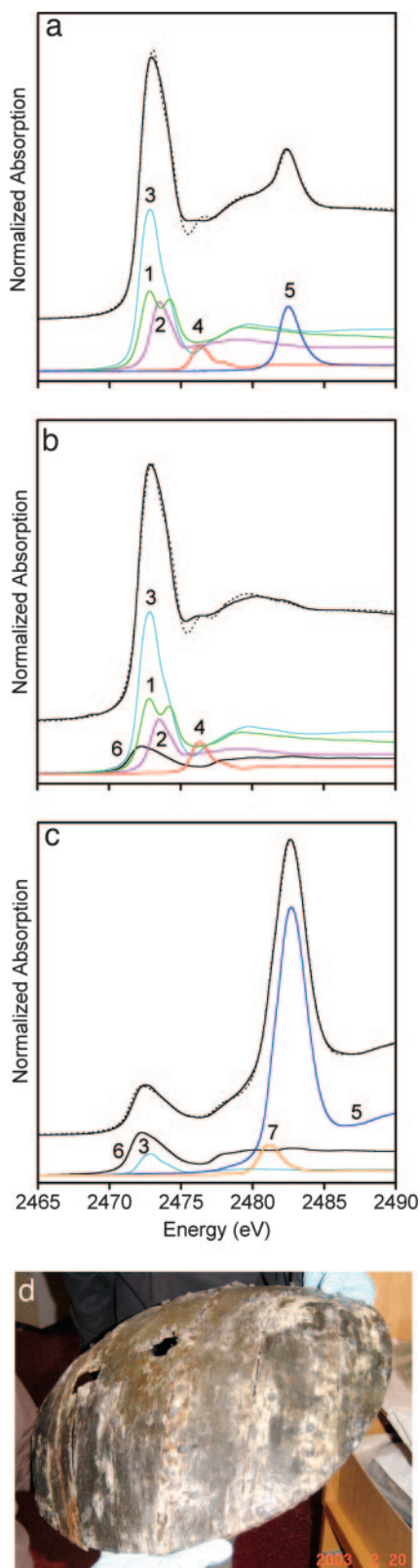


Fig. 4. XANES evaluation of sulfur species by fitting linear combinations of standard spectra. (a) Core 1a (0–5 mm): 1, disulfides R–SS–R' 31 atom % S; 2, thiols R–SH 23%; 3, elemental sulfur S_8 36%; 4, sulfoxide R_2SO [or $R(SO)R'$] 4%; 5, sulfate SO_4^{2-} 6%. (b) Core 2 (15–17 mm): 1, R–SS–R' 29%; 2, R–SH 18%; 3, S_8 35%; 4, R_2SO 5%; 6, pyrite FeS_2 13%. (c and d) Wooden remains of a gun shield from the *Mary Rose* with salt formation on the surface (see photo, d): 3, S_8 6%; 5, sulfate 63% (standard: melanterite $FeSO_4 \cdot 7H_2O$); 6, FeS_2 26%; 7, sulfonate $R-SO_3^-$ 5%.

Table 1. XANES analysis of the relative amount of sulfur species at various depths in oak core 2 from hull timber

Depth, mm	FeS_2	S_8	R–SH	RSSR'	R_2SO
16	12	35	18	29	6
56	0	47	20	27	6
78	19	31	11	33	6
114	22	26	13	33	6
133	0	36	24	35	5

The total sulfur concentration varies from 0.5 to ≈ 1.5 mass % S along the core with iron fluctuating up to ≈ 1 mass % (Fig. 2). The amount of oxidized S(VI) species is negligible (no peak at $\approx 2,483$ eV in Fig. 3b).

cellulose (12, 13), and the variations indicate that pockets or zones of decayed wood extend throughout the *Mary Rose* timbers and facilitated penetration in the waterlogged wood consistent with the relatively uniform sulfur concentration profiles (Figs. 2 and 12).

Formation of Sulfur Compounds

The near anoxic environment that slows down degradation of waterlogged wood normally occurs at or below the seafloor, where bacteria metabolizing organic debris reduce sulfate ions to hydrogen sulfide, H_2S (13, 20). Evidently, dissolved hydrogen sulfide penetrates and reacts to solid reduced sulfur compounds within the waterlogged wood in amounts depending on the state of wood degradation, the concentration of hydrogen sulfide, and also iron(II) ions from corroding iron. This conclusion is illustrated by the distribution of sulfur compounds in wood from shipwrecks preserved under different conditions. In the *Vasa* the bacterially degraded surface layer shows high accumulation that in several cases exceeds 10 mass % S and Fe (4–8); in the *Mary Rose* all analyzed cores, except for the iron-rich gun shield, show a fairly uniform concentration at ≈ 1 mass % S while iron fluctuates, and core samples from the *Bremen Cog* from 1380 are very low both in sulfur and iron, <0.2 mass % (9). Around the exposed hull of the *Vasa* the increasingly polluted brackish water in the Stockholm harbor occasionally reached very high concentrations of hydrogen sulfide for centuries before the salvage (8); the *Mary Rose* timbers were covered by clay restricting the circulation of the anoxic seawater (1–3), whereas the *Bremen Cog* was preserved covered by clay in river water, which has low sulfate concentration and consequently low bacterial production of hydrogen sulfide (9). The iron and sulfur concentration profiles, obtained by high-resolution x-ray fluorescence line scans along cores, often follow each other closely for the *Vasa* (8, 9), indicating that initially iron sulfides were formed when dissolved hydrogen sulfide and iron(II) ions penetrated the exposed waterlogged wood.

One important issue for stable conservation is how accessible and reactive the sulfur compounds are to acid-producing oxidation in an aerobic environment. Therefore, we examined thin wood slices (a few micrometers) cut with razor blades perpendicular to the cell walls by scanning x-ray absorption microspectroscopy (SXM) at beamline ID21 of the European Synchrotron Radiation Facility (21, 22). The SXM microprobe, operated under low-grade vacuum to avoid the strong air absorption, enabled mapping of sulfur species with a spectral resolution of 0.5 eV over sample areas up to $100 \times 100 \mu m$ at high spatial resolution, $\approx 0.5 \mu m$. Raster scanning of the sample in the focused beam was performed at energies of characteristic sulfur XANES resonances, $\approx 2,473$ and 2,483 eV, to obtain the distributions of reduced and oxidized sulfur species, respectively.

The SXM images obtained of oak wood from hull timber at the x-ray energy 2,473 eV consistently reveal reduced sulfur species in high concentration in lignin-rich parts, especially in the middle

Table 2. Multielement x-ray photoelectron spectroscopy analyses of core 1b and a surface sample from the gunshield

Depth, mm	Total S	S reduced*	Sulfoxide	Sulfate	Fe	C	O	B
7.5	0.78	0.68 (87%)	0.04	0.05	0.20	27.2	6.4	0.17
10	0.66	0.56 (85%)	0.03	0.08	0.19	27.1	6.8	0.19
15	0.89	0.77 (87%)	0.05	0.07	0.17	26.0	7.5	0.18
33	0.81	0.71 (88%)	0.05	0.05	0.06	26.6	7.2	0.14
34	0.74	0.66 (89%)	0.03	0.05	0.18	31.7	2.3	0.05
45	0.70	0.60 (86%)	0.06	0.04	0.21	30.0	4.0	0.12
60	0.64	0.58 (89%)	0.04	0.05	—	24.4	10.0	0.13
75	0.64	0.51 (80%)	0.05	0.08	0.28	26.5	7.5	0.14
89	0.69	0.63 (91%)	0.07	0.03	0.02	23.2	11.0	0.19
92.5	0.77	0.49 (61%)	0.12	0.16	0.4	26.8	7.0	0.07
99	0.68	0.59 (87%)	0.05	0.05	0.14	23.5	10.1	0.11
104	0.65	0.50 (77%)	0.07	0.08	0.51	29.8	4.0	0.09
112	0.72	0.54 (67%)	0.08	0.09	0.34	28.2	5.6	0.11
144	0.80	0.70 (87%)	0.03	0.07	—	23.8	10.3	0.26
Gunshield	3.5	0.60 (17%)	0.07	2.8	2.8	16.3	13.2	—

Values are in mass %. The mass % scale was obtained by assuming two hydrogen atoms per carbon.

*Values in parentheses represent the percentage of sulfur in reduced species.

lamella between the wood cells. The lignin-reinforced walls of a vessel in freshly salvaged oak wood even display a distinct double layer (Fig. 6 and 8). Complementary studies by means of scanning electron microscopy (SEM) and x-ray fluorescence elemental analysis showed sulfur but no iron in the middle lamella (8, 9).

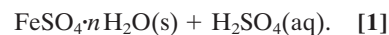
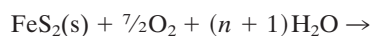
The SXM microprobe also allows focused micro-XANES spectra to be measured. Such spectra from submicrometer spots in the middle lamella are consistent with sulfur in thiols at the peak energy 2,473 eV, as for the unfocused SSRL XANES spectra of higher signal-to-noise (cf. Figs. 4 and 6a, spot 2). The high concentration of organosulfur in lignin-rich parts indicates direct reaction of the hydrogen sulfide (or HS[−] ions) with active sites in lignin, e.g., activated double bonds (ref. 23 and references therein) and probably also ether, carbonyl, and α -hydroxy groups. This finding resembles the early diagenetic formation of

organosulfur species in humic matter and carbohydrates (20, 23–27). Sulfur uptake in lignin has geochemical significance for anoxic marine sediments, where cross-linking of thiols with S–S bonds are proposed to build macromolecular structures within humic substances (partly composed of lignin) and may enhance the preservation of the organic matter (25, 27).

The Role of Iron

Corroding bolts, nails, and other objects of mild steel primarily form soluble iron(II) ions, which can successfully compete with organic substances for hydrogen sulfide and react to iron sulfides (Fe_{1-x}S and pyrite) (24, 26, 28). The XANES spectra indicate that in the waterlogged wood, in addition to the thiols and disulfides in lignin-rich parts, pyrite (Table 1) and other iron sulfides form when iron(II) ions can penetrate (Figs. 3 and 4). Micro-XANES sulfur spectra of particles in wood cavities (vessels and lumina) occasionally show peaks at energies as low as \approx 2,470 eV (cf. Fig. 6a, spectra 1 and 3) that are characteristic of sulfides with some amount of iron(III), such as pyrrhotite (Fe_{1-x}S) or greigite (Fe₃S₄).

Iron sulfides are known to oxidize in a humid environment (29, 30) and are probably the primary source of the acid forming in the hygroscopic PEG impregnated marine-archaeological wood. Thermodynamically, the stepwise oxidation process of iron sulfides ends at sulfate and releases acid, as for pyrite (29):



Acid has continuously been washed out during the 10 years of spraying the *Mary Rose* hull. To keep the pH of the recycled conservation liquid neutral, 0.8 tons of sodium bicarbonate has been added so far. For the *Vasa*, 5 tons of borax, Na₂B₄O₇·10H₂O(s), was added as fungicide during 13 years of recirculation (10); an amount sufficient to neutralize \approx 1.3 tons of sulfuric acid (5, 6). The acid that has formed during the 26 years after the spray treatment was stopped in 1979, and now is present in the *Vasa*'s hull timbers, is estimated to correspond to \approx 2 tons of sulfuric acid (4, 6–8).

Iron contamination of marine-archaeological wood is a well-known preservation concern (3). With oxygen access to moist PEG impregnated wood, iron compounds can catalyze oxidation processes, e.g., oxidation of sulfides and reduced

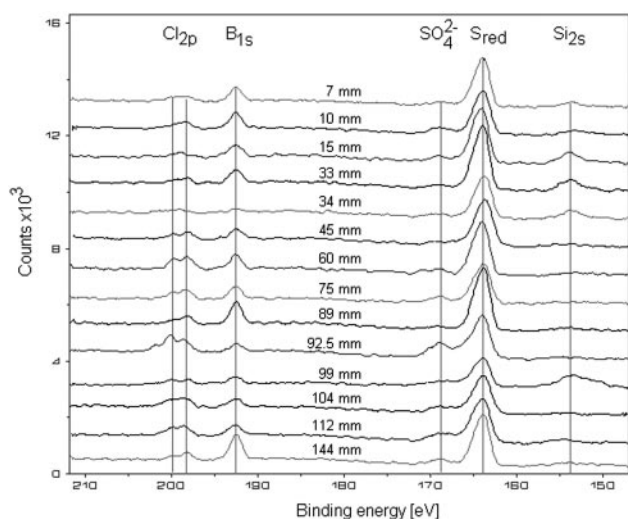


Fig. 5. X-ray photoelectron spectra of oak core 1b (cf. Table 2). The vertical lines mark binding energies in the energy range 150–210 eV of the element-specific photoelectrons Cl_{2p}, B_{1s}, S_{2p}, and Si_{2s}. The mean S 2p_{3/2} binding energies were 163.7 and 168.8 eV for the reduced (S_{red}) and oxidized (S_{ox}) sulfur species, respectively. Cracks in the core correspond to increased intensities of the chloride and sulfate peaks.

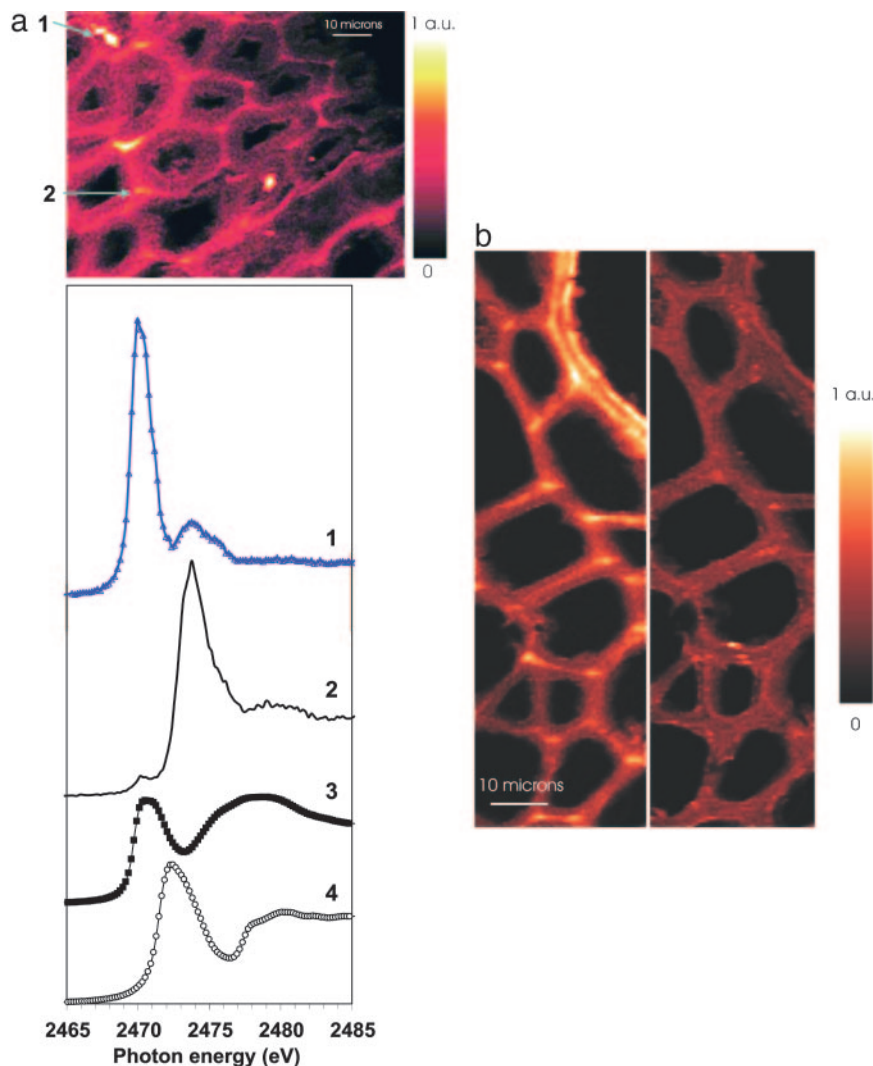


Fig. 6. SXM images at 2,473 eV (higher reduced sulfur concentration \rightarrow brighter color) and micro-XANES of oak wood from the *Mary Rose*. (a Upper) Hull timber under spray treatment shows reduced sulfur accumulated in middle lamella. (Lower) The micro-XANES curves correspond to 1, bright particle; 2, middle lamella; 3, pyrrhotite $4C(Fe_{1-x}S)$ as standard; and 4, pyrite FeS_2 as standard. (b) Freshly salvaged (in 2004) oak wood from the *Mary Rose* after 459 years on the seafloor. (Left) The SXM image at 2,473 eV displays two layers of thiols in high concentration in the lignin-rich cell wall of a vessel (top right), which is a channel for water flow in oak wood (cf. Fig. 8); the dark patches surrounded by cell walls are the lumina. (Right) The 2,483 eV image shows a few bright sulfate particles.

sulfur compounds to sulfuric acid (29, 30), but also can direct oxidative degradation of cellulose and probably successive degradation of the PEG polymers through formation of hydroxyl radicals. Practical tests of methods to dissolve and remove iron(III) compounds, and at the same time neutralize acid, are being carried out on marine-archaeological wood in the "Preserve the *Vasa*" project (6, 8). Such chemical processes are usually not compatible, because iron(III) oxyhydroxides (rust) precipitate already at low pH from aqueous solutions. However, derivatives of the well-known chelate EDTA can be tailored to enclose the small iron(III) ions with six efficient donor atoms arranged in a well-fitting cage (6, 7). Such a chelating agent is EDMA, ethylenediiminobis(2-hydroxy-4-methyl-phenyl) acetic acid, forming particularly strong bonds in a complex $[Fe(EDMA)]^-$, which was developed as a water-soluble iron micronutrient to increase productivity of citrus tree plantations on carbonate rich alkaline soils (31). For marine-archaeological wood, microspectroscopy (SXM, SEM) will be useful to assess the efficiency of the iron-extraction treatments with EDMA and to evaluate the removal of specific sulfur compounds (SXM).

Long-Term Conservation Requirements

Our current working hypothesis is that, after removing or making reactive iron species inert as oxidation catalysts, e.g., by EDMA treatment, the remaining lignin-bonded organosulfur could be prevented from forming acid in the marine-archaeological wood. To exhaust the strongly acid-forming iron sulfides more rapidly during a spray treatment period, mild oxidation by singlet oxygen (1O_2), generated by UV radiation in the conservation liquid and carried by dissolved organic material (30), could be tested. Also, raised temperature would accelerate the oxidation process, although careful control of microbial activity (especially *Legionella*) then must be asserted (3). However, attempts at gentle sulfur extraction or selective oxidation by sulfur-oxidizing bacteria do not appear useful for removing the organosulfur in the middle lamella. For the *Mary Rose* timbers, the rate of further acid production will be carefully monitored to appraise a suitable end point of the current spray treatment.

For acid-free PEG treated marine-archaeological wooden artifacts, a stable museum climate with small variations in

temperature and relative humidity (preferably $\approx 55\%$ relative humidity) is a primary requirement to enable long-term conservation. Enclosure or coatings to reduce oxygen access also could be considered to slow down degrading reactions. The international “Preserve the *Vasa*” project, started in late 2003, aims at developing suitable methods to neutralize the acid that may continue to form in marine-archaeological wooden artifacts after traditional PEG conservation treatment and to remove or stabilize remaining sulfur and iron compounds (6).

We thank the participants in the Preserve the *Vasa* project for many stimulating discussions, especially Dr. Ingmar Persson for comments on EDMA extraction and PEG stability. We thank the European Synchrotron Radiation Facility and SSRL for generously allocating beamtime and Dr. Patrick Frank (SSRL) for providing an insight in

fitting sulfur XANES spectra. This work was supported by grants from the Knut and Alice Wallenberg Foundation, the Carl Trygger Foundation, and the “Preserve the *Vasa*” project at the National Maritime Museums of Sweden, sponsored by The Bank of Sweden Tercentenary Foundation, the Swedish National Heritage Board, Swedish Foundation for Strategic Research (SSF), the Swedish Research Council for Environment, Agricultural Sciences and Spatial Planning (FORMAS), and the Swedish Agency for Innovation Systems (VINNOVA). F.J. is the recipient of a University Faculty Award with financial support by the Natural Sciences and Engineering Research Council of Canada. SSRL is a national user facility operated by Stanford University on behalf of the U.S. Department of Energy, Office of Basic Energy Sciences. The SSRL Structural Molecular Biology Program is supported by the Department of Energy, Office of Biological and Environmental Research, and by the National Institutes of Health, National Center for Research Resources, Biomedical Technology Program.

1. Marsden, P. (2003) *Sealed by Time: The Loss and Recovery of the Mary Rose*, The Archaeology of the *Mary Rose* (The *Mary Rose* Trust, Portsmouth, U.K.), Vol. 1.
2. Rule, M. (1982) *The Mary Rose. The Excavation and Raising of Henry VIII's Flagship* (Conway Maritime Press, London).
3. Jones, M. (2003) in *For Future Generations: Conservation of a Tudor Maritime Collection*, The Archaeology of the *Mary Rose*, ed. Jones, M. (The *Mary Rose* Trust, Portsmouth, U.K.), Vol. 5.
4. Sandström, M., Jalilehvand, F., Persson, I., Gelius, U., Frank, P. & Hall-Roth, I. (2002) *Nature* **415**, 893–897.
5. Sandström, M., Jalilehvand, F., Persson, I., Gelius, U. & Frank, P. (2002) in *Proceedings of the Eighth ICOM Group on Wet Organic Archaeological Materials Conference, Stockholm, 2001*, eds. Hoffmann, P., Spriggs, J. A., Grant, T., Cook, C. & Recht, A. (Deutsches Schiffahrtsmuseum, Bremerhaven, Germany), pp. 67–89.
6. Sandström, M., Fors, Y. & Persson, I. (2003) *The Vasa's New Battle: Sulfur, Acid and Iron*, Vasa Studies (Vasa studies 19, The Vasa Museum, Stockholm, Sweden), Vol. 19.
7. Sandström, M., Jalilehvand, F., Persson, I., Fors, Y., Damian, E., Gelius, U., Hall-Roth, I., Dal, L., Richards, V. L. & Godfrey, I. (2003) in *Conservation Science 2002*, eds. Townsend, J. H., Eremin, K. & Adriaens, A. (Archetype Books, London), pp. 79–87.
8. Fors, Y. (2005) Licentiate Thesis (Structural Chemistry, Stockholm University, Stockholm).
9. Sandström, M., Fors, Y., Jalilehvand, F., Damian, E. & Gelius, U. (2005) in *Proceedings of the Ninth ICOM Group on Wet Organic Archaeological Materials Conference, Copenhagen, 2004*, ed. Hoffmann, P. (Deutsches Schiffahrtsmuseum, Bremerhaven, Germany), in press.
10. Häfors, B. (2001) *Conservation of the Swedish Warship Vasa from 1628*, Vasa Studies (The Vasa Museum, Stockholm), Vol. 18.
11. Gelius, U., Wannberg, B., Baltzer, P., Fellner-Feldegg, H., Carlsson, G., Johansson, C.-G., Larsson, J., Münger, P. & Vegerfors, G. (1990) *J. Electron Spectrosc. Relat. Phenom.* **52**, 747–785.
12. Blanchette, R. A., Nilsson, T., Daniel, G. & Abad, A. (1990) in *Archaeological Wood: Properties, Chemistry and Preservation*, Advances in Chemistry Series, eds. Rowell, R. M. & Barbour, R. J. (Am. Chem. Soc., Washington, DC), Vol. 225, pp. 141–192.
13. Björkdal, C. (2000) Ph.D. thesis (Swedish University of Agricultural Sciences, Uppsala, Sweden).
14. Hedman, B., Frank, P., Penner-Hahn, J. E., Roe, A. L., Hodgson, K. O., Carlson, R. M. K., Brown, G., Cerino, J., Hettel, R., Troxel, T., et al. (1986) *Nucl. Instr. Methods A* **246**, 797–800.
15. Pickering, I. J., Prince, R. C., Divers, T. & George, G. N. (1998) *FEBS Lett.* **441**, 11–14.
16. Pickering, I. J., George, G. N., Yu, E. Y., Brune, D. C., Tuschak, C., Overmann, J., Beatty, J. T. & Prince, R. C. (2001) *Biochemistry* **40**, 8138–8145.
17. George, G. N., George, S. J. & Pickering, I. J. (2001) EXAFSPAK: *Computer Program Package* (Stanford Synchrotron Radiation Laboratory, Menlo Park, CA).
18. Sarret, G., Connan, J., Kasrai, M., Bancroft, G. M., Charrié-Duhaut, A., Lemoine, S., Adam, P., Albrecht, P. & Eybert-Bérard, L. (1999) *Geochim. Cosmochim. Acta* **63**, 3767–3779.
19. Damian, E., Jalilehvand, F., Abbasi, A., Pettersson, L. G. M., Sandström, M. (2005) *Phys. Scripta* **T115**, 1077–1079.
20. Sinninghe Damsté, J. S. & de Leeuw, J. W. (1990) *Adv. Org. Geochem.* **16**, 1077–1101.
21. Susini, J., Salomé, M., Fayard, B., Ortega, R. & Kaulich, B. (2002) *Surf. Rev. Lett.* **9**, 203–211.
22. David, C., Kaulich, B., Barrett, R., Salomé, M. & Susini, J. (2000) *Appl. Phys. Lett.* **77**, 3851–3853.
23. Vairavamurthy, M. A., Maletic, D., Wang, S., Manowitz, B., Eglinton, T. & Lyons, T. (1997) *Energy Fuels* **11**, 546–553.
24. Passier, H. F., Böttcher, M. E. & De Lange, G. J. (1999) *Aq. Geochem.* **5**, 99–118.
25. Xia, K., Weesner, F., Bleam, W. F., Bloom, P. R., Skjellberg, U. L. & Helmke, P. A. (1998) *Soil Sci. Soc. Am. J.* **62**, 1240–1246.
26. Dellwig, O., Watermann, F., Brumsack, H.-J., Gerdes, G. & Krumbein, W. E. (2001) *Palaeogeogr. Palaeoclimatol. Palaeoecol.* **167**, 359–379.
27. van Dongen, B. E., Schouten, S., Baas, M., Geenevasen, J. A. J. & Sinninghe Damsté, J. S. (2003) *Org. Geochem.* **34**, 1129–1144.
28. Butler, I. B. & Rickard, D. (2000) *Geochim. Cosmochim. Acta* **64**, 2665–2672.
29. Jerz, J. K. & Rimstidt, J. D. (2004) *Geochim. Cosmochim. Acta* **68**, 701–714.
30. Stumm, W. & Morgan, J. (1996) *Aquatic Chemistry: Chemical Equilibria and Rates in Natural Waters* (Wiley, New York), 3rd Ed., Chapters 11 and 12.
31. Ahrlund, S., Dahlgren, Å. & Persson, I. (1990) *Acta Agric. Scand.* **40**, 101–111.